American Mineralogist, Volume 78, pages 957–967, 1993

Single-crystal absorption and reflection infrared spectroscopy of birefringent grossular-andradite garnets

B. P. McAloon, A. M. Hofmeister
Department of Geology, University of California, Davis, California 95616, U.S.A.

Abstract

Reduction in symmetry of optically anomalous garnets from $Ia\bar{3}d$ to $I\bar{1}$ or $Fddd$ by cation ordering, as indicated by crystallography, implies that a large number of vibrations (129 or 98) should be infrared (IR) active. Yet, only the pattern characteristic of isotropic isometric garnets was observed in single-crystal polarized and unpolarized IR reflectance spectra from 80 to 4000 cm^{-1} of four birefringent garnets ($Gr_{90}An_6Al_4$, $Gr_{99}An_1$, $An_{94}Gr_5Sp_1$, and $Gr_{60.8}An_{36.5}Sp_{1.3}Al_1Py_{0.3}$). These samples are nearly identical to those whose structures have been crystallographically refined. We also present the first single-crystal IR absorption spectrum that resolves the entire fundamental region and find this compares closely with data from reflection measurements. An extra band seen near 690 cm^{-1} is attributed to an overtone because it is present in isotropic garnets. The absence of orientational dependence and existence of 17 (or fewer) IR fundamentals (rather than the 98–129 expected) is consistent with an $Ia\bar{3}d$ space group: ordering of divalent or trivalent cations is not apparent. The contrasting results from spectroscopy and crystallography may indicate that strain causes anomalous optical anisotropy in garnet (as occurs in diamond and quartz) in that X-ray diffraction requires juxtaposition of ~1000 unit cells, whereas lattice vibrations can be produced by isolated molecules.

Introduction

Although the isometric symmetry of garnets would ordinarily require optical isotropy, grossular-andradite garnets from skarns commonly exhibit weak birefringence. One possible origin for their anomalous optical properties is the reduction of symmetry through partial ordering of Al and Fe^{3+} in the octahedral sites (or of Ca and Fe^{2+} in the dodecahedral sites), as indicated by crystallographic refinements (Takéuchi et al., 1982; Allen and Buseck, 1988; Kingma and Downs, 1989; Griffen et al., 1992). Infrared (IR) spectroscopic analysis of such low-symmetry garnets presents a unique opportunity to study vibrational modes that are inactive in the cubic structure. Such data would improve the accuracy of thermodynamic calculations (Kieffer, 1979) useful for geothermometry and geobarometry.

This paper presents single-crystal absorption and reflection IR spectra (polarized and unpolarized) obtained from optically oriented sections of four birefringent garnet samples similar to those crystallographically refined. The IR data implicate the isometric garnet structure. This surprising result precludes improvement of the thermodynamic models. The apparent contradiction between IR results and previous crystallographic refinements (Takéuchi et al., 1982; Allen and Buseck, 1988; Kingma and Downs, 1989) may pertain to the origin of birefringence in garnet.

Experimental

Four samples were studied: andradite ($An_{94}Gr_5Sp_1$) from the Sonoma Mountain Range, Nevada, supplied by K. J. Kingma and J. W. Downs; grossular from Asbestos, Quebec, Canada ($Gr_{99}An_1$), and Eden Mills, Vermont ($Gr_{90}An_6Al_4$), provided by F. M. Allen and P. R. Buseck; and grandite from Munam, North Korea ($Gr_{60.84}$-$An_{36.50}Sp_{1.33}Al_{1.00}Py_{0.33}$), provided by G. R. Rossman. Takéuchi et al. (1982), Allen and Buseck (1988), Kingma and Downs (1989), and Rossman and Aines (1991) gave sample descriptions.

For reflectance studies, single crystals ranging from ~0.25 × 0.25 × 0.03 to ~6.5 × 5.0 × 0.5 mm were singly polished (Figs. 1–5[1]). For absorbance studies, the andradite was doubly polished and thinned to <10 μm over areas of ~0.8 mm^2 using a Gatan model 656/3 Dimple Grinder. Grossular samples roughly 5 mm in diameter were doubly polished to a thickness of approximately 30 μm and then ion thinned (Tighe, 1976) to about 0.5–2.0 μm using a Gatan model 600 Dual Ion Mill. Ion thinning is preferred to dimpling because uniform thinning is achieved over a greater surface area and detaching

[1] A copy of Figures 1–5 and Tables 1–5 may be requested from the authors or ordered as Document AM-93-535 from the Business Office, Mineralogical Society of America, 1130 Seventeenth Street NW, Suite 330, Washington, DC 20036, U.S.A. Please remit $5.00 in advance for the microfiche.

0003–004X/93/0910–0957$02.00

TABLE 6. Infrared data for grossular-andradite

		Andradite, Sonoma				Andradite, Santa Rita**		Impure andradite†	Impure andradite‡	Grandite, Munam		Grossular, asbestos	
		Reflectance		Single-crystal absorption		Reflectance		Transmission Powder	Transmission Powder	Reflectance		Reflectance	
No.*	Assignment**	LO	TO	LO	TO	LO	TO	position	position	LO	TO	LO	TO
1B	ν_3	988.0	884.6	974	881.8	970	875.6	888	880	1000.3	900.3	1007.4	907.8
3C	ν_3	823.8	830.5		815	819	821.8	831	840	843	845	851.4	856.3
4D	ν_3	861.6	811.9		805(?)	858	795.3	811	—	878.0(2)	825.6	884.7	837.7
7E	ν_4	594.6	590.7		590.7	592	588.4	589	599	612.0(2)	607.8	623.8	618.0
9F	ν_4	536.1	510.6		509.9	532	505.3	510	514	558.4(4)	529.2	576.2	539.8
10G	ν_4	488.3	480.3		479.1	487	478.8	477	480	494	494	506	506
13I	ν_2	461.3	435.2		~428	460	432.7	438	440	510.8	419.8	529.4	434.9
15K	$R(SiO_4)$	419.9	378.6	403	~372	418	374.1	390	—	390.6	377.5	404.9	389.8
18L	$R(SiO_4)$	~323	324		~320	322	323.7	330 sh	—	354(2)	346(2)	356	355
19H	T_o	359.5	351.6		~350	358.5	349.7	352	352	456.9	459.2	469.5	470.6
20J	T_o	332.5	301.0		~290	332	295	309 br	304 br	—	—		~430§
21N	T_o	134.7	133.7		133.3	133.5	132.8	133	132	200.5	197	248.7	241.4
22O	T_d	247.5	246.4		246.2	246	246.6	245	—	238.3	232.7	248.7	241.4
23P	T_d	216.7	214		214.5	215	213.4	211	212	200.5	197	207.4	204.5
24Q	T_d	192.1	188.4		188	192	187.6	186, 113‖	185, 112‖	175	172.4	188.8	184
27M	$T(SiO_4)$	~284	~279		278.9	~300	~305	—	—	292.8	288	302.9	300.6
29R	$T(SiO_4) + T_d$	154.2	153		152	154	152.1	155	151	147.6	146.7	157.5	155.6
i	overtone	—	—		648	—	—	690	704	752.5	751.9	—	—
ii	overtone		939	—	—	—	—	929	1070		~956		~972

Note: all frequencies in wavenumbers; sh = shoulder; br = broad.

* Nomenclature after Tarte (1965), Moore et al. (1971), Hofmeister and Chopelas (1991).

** Data from Hofmeister and Chopelas (1991).

† Data from Moore et al. (1971) on $An_{94}Gr_{4.5}Py_{1.2}Sp_{0.5}$. Similar spectra were obtained from An_{93} with almandine and grossular components.

‡ Data from Madon et al. (1991) on a pale green andradite. Pure andradite is yellow, suggesting that Fe^{2+} or Cr^{3+} was present.

§ Estimated frequency, inferred to be degenerate with 13I (see text).

‖ Two mode behavior resulting from almandine or spessartine component.

the sample from the sample mount is unnecessary, which reduces the risk of sample breakage.

IR spectra were obtained at ambient conditions using a Bomem DA3.02 Fourier-transform interferometer and a Spectra-Tech FTIR microscope. An image mask was used for samples smaller than the field of view (600 μm), and reference spectra were obtained under the same conditions. Wire grids were used to obtain measurements polarized at 0 and 90°, relative to extinction directions, from optically oriented samples. Departure from near-normal incidence owing to the convergent optics of the microscope has some influence on peak positions and intensity. As demonstrated through classical dispersion analysis (e.g., Spitzer et al., 1962), which includes the effect of the incidence angle (Jackson, 1975), the S polarization gives slightly broader and taller peaks by several percent, but the P polarization gives the opposite, whereas unpolarized data are not affected by non-normal incidence. The possibility of such minor differences in polarized compared with unpolarized data owing to convergent optics is considered in the results section.

Far-IR spectra were obtained at a resolution of 1 or 2 cm^{-1} from about 90 to >500 cm^{-1} using a liquid-He cooled silicon bolometer (Infrared Laboratories, Tucson, Arizona), whereas mid-IR spectra were obtained at a resolution of 1 or 2 cm^{-1} from about 450 to 4000 cm^{-1} using a HgCdTe detector cooled with liquid N_2. A Kramers-Kronig analysis (Andermann et al., 1965) was performed on the merged mid- and far-IR reflectance data. For details see Hofmeister and Chopelas (1991). Uncertainty in peak positions of ± 0.1–0.01 cm^{-1} are related to breadths of the bands because the accuracy of the spectrometer is two orders of magnitude smaller.

SYMMETRY ANALYSIS

The garnet structure consists of a three-dimensional network of alternate corner-linked tetrahedra and octahedra, both of which share edges with larger cations in dodecahedrally coordinated interstices (Euler and Bruce, 1965; Novak and Gibbs, 1971). This O_h^{10} isometric structure has 17 triply degenerate T_{1u} modes that are active in the infrared region, and 25 Raman and 45 inactive modes of various degeneracies (Hurrell et al., 1968). If the vibrations of the isolated tetrahedra are only mildly perturbed by placing them in the garnet structure, then the 17 IR modes should consist of three asymmetric stretching modes, ν_3, of the tetrahedron, three asymmetric bends, ν_4, one symmetric bend, ν_2, two rotations (librations), R, of the tetrahedron, two translations, T, of the tetrahedron, three translations, T_d, of the dodecahedral cations, and three translations, T_o of the octahedral cations (e.g., Moore et al., 1971). This description is valid to a first approximation, as shown by several lines of evidence (Hofmeister and Chopelas, 1991; and references therein; Lu et al., 1993; and references therein) and is used to correlate bands between garnets of varying chemistry.

Reduction in symmetry necessarily increases the number of bands active in both the infrared and Raman sym-

TABLE 6.—*Continued*

Grossular, asbestos		Grossular, Eden Mills				Grossular, Jeffrey mine**	
Single-crystal absorption		Reflectance		Single-crystal absorption		Reflectance	
LO	TO	LO	TO	LO	TO	LO	TO
995	910	1011.1	909.2	995	909	1010	914
	859.9	852.3	856.8		855	850	860.2
	833.3	886.2	836.8		835	883	842.8
	617.3	623.6	617.8		616	631	618.3
572	540.6	577.8	540.5	569	539.4	579	541.8
—	—	505.7	504.2		502.6	503	505
	430	528.0	436.8		~435	530	448.7
	387.5	404.9	391.8		389.9	406	398.5
	353.2	356.7	357.5		355.7	357	356
—	—	469.1	471.4		469.5	468	473.5
—	—		~420§		~430§	~425	~430
	240.6	248.0	240.9		238.1	249	244.6
	240.6	248.0	240.9		238.1	249	244.6
	203.8	205.9	202.9		201.4	207	205.4
	183	186.8	183.3		180.6	189	186
	298.1	302	300.1		296.9	303	301.6
	154.9	158.3	156.5		154.9	159	158.6
	689		699?		776	—	—
—	—		968	—	—	—	—

metries through a relaxation of selection rules and the lifting of degeneracies in the nonisometric cell. Optic modes of the orthorhombic structure *Fddd,* indicated for North Moravia and Kamaishi garnets (Takéuchi et al., 1982), are distributed as

$$25A_g\,(R) + 27B_{1g}\,(R) + 28B_{2g}\,(R) + 28B_{3g}\,(R) + 31A_u + 32B_{1u}\,(I) + 33B_{2u}\,(I) + 33B_{3u}\,(I), \quad (1)$$

where I indicates IR activity and R indicates Raman activity. The triclinic structure $I\bar{1}$ has a larger number of bands:

$$108A_g\,(R) \text{ and } 129A_u\,(I). \quad (2)$$

Tables 1 and 2[1] give details of these calculations.

Three paths are allowed for the ordering of cations on the octahedral or dodecahedral sites (Hatch and Griffen, 1989). The most symmetrical structures along each of these paths have >50 IR modes apiece (see Tables 3–5[1]). Thus any type of ordering should drastically increase the number of IR active peaks.

Symmetry analysis predicts the number of modes, given that all frequencies are distinct. Accidental degeneracies can reduce the number of peaks observed, and overtones and impurities can increase this. In general, the number of modes observed is ±0, 1, or 2 from that expected if single-crystal spectra are acquired (see examples in McMillan and Hofmeister, 1988). We also note that the width of an IR fundamental is proportional to its intensity (see e.g., Spitzer et al., 1962; Wooten, 1972); hence, the weak peaks expected from reduction in symmetry will be sharp and thus should be readily observable.

RESULTS

Both unpolarized and polarized reflectance spectra were obtained to establish positions and numbers of IR peaks. Samples with nonisometric symmetry are expected to show a variation in number and position of peaks between these two types of measurements. Absorbance spectra were obtained in order to establish the possible presence of weak IR modes, which can be obscured by intense bands. Spectra from different zones within each sample were examined to test for spatial variations. Efforts were concentrated on the Eden Mills grossular, which showed spectacular optical birefringence (Figs. 3, 4). For the Munam garnet, spatial information was not sought because the extinction pattern was uniform across the sample. This solid-solution grandite is of particular interest because ordering in the octahedral or dodecahedral sites, should it occur, would be found in most unit cells, as opposed to ordering for near end-members, which would occur in fewer than one-tenth of the unit cells.

Unpolarized reflectance

Unpolarized reflectance spectra from all four birefringent samples (Fig. 6) show patterns characteristic of isometric garnets (Hofmeister and Chopelas, 1991): that is, 17 IR modes for andradite and 15 IR modes for grossular, which has one accidental degeneracy at 241 cm^{-1} and one very weak shoulder near 430 cm^{-1}. The only differences between the birefringent garnets of this study and optically isotropic garnets of Hofmeister and Chopelas (1991) are in the resolution of shoulders, occasional noise, and relative intensity of the far-IR and mid-IR bands. The latter variation is due to a small overlap (~50 cm^{-1}) between the spectral regions in the previous study, which could contribute to slight frequency differences. No evidence was seen for the additional modes expected for lower symmetries. The longitudinal optic (LO) and transverse optic (TO) values from these four garnet samples (Table 6) closely match those observed for optically isotropic grossular and andradite by Hofmeister and Chopelas (1991). Slight differences (±5 cm^{-1}) could be associated with minor differences in composition. Data from the present study are more accurate because (1) absolute reflectivity was established by acquiring reference spectra under the same conditions used to collect sample data, (2) the overlap between mid- and far-IR regions is larger in the present study (~100 cm^{-1}), and (3) the signal to noise ratio is higher.

No spatial effect was seen. Only trivial differences exist among the unpolarized spectra (Fig. 7) taken from various zones within the Asbestos and Eden Mills grossular and the andradite (Figs. 1–4). The mid- and far-IR data for the Munam grandite were measured from different areas of the sample (Fig. 5), but no differences from the

isometric garnet pattern were seen that would suggest spatial variations.

Peak positions for the weak shoulders in the Sonoma andradite (modes 18L and 27M, Table 6) are approximate, whereas all other peaks are well resolved (Fig. 6a). Peak values were established from polarized studies for the region from ~550 to 690 cm^{-1} of andradite because of their low noise level. All 17 peaks are accounted for, and differences with optically isotropic Santa Rita andradite are minimal.

Asbestos grossular has 15 distinct reflectance peaks (Fig. 6b). Inspection of the dielectric function ϵ_2 and $Im(1/\epsilon)$ [the imaginary part of $1/(\epsilon_1 + i\epsilon_2)$] obtained through Kramers-Kronig analysis shows that the poorly resolved shoulder seen near ~430 cm^{-1} is probably not an artifact. That mode 20J in Table 6 is a fundamental is suggested by the asymmetry of the main peak at 432 cm^{-1} in both ϵ_2 and in $Im(1/\epsilon)$, by the offset in the base line of the ϵ_1 dielectric function, and by trends in the series $X_3Al_2Si_3O_{12}$ (Hofmeister and Chopelas, 1991).

Large crystals of Jeffrey mine grossular are birefringent; however, the number of peaks and relative intensities of both Raman and IR bands of this grossular are remarkably similar to those found for pyrope, almandine, and spessartine (Hofmeister and Chopelas, 1991). The major spectral changes are found in frequency shifts for the low-lying peaks and are correlated with substitution of the dodecahedral cation (Mg, Fe, Mn, or Ca). Also, peak shifts in this series show a linear dependence on volume. The consistent trends, similar intensities, and number of bands all point to the $Ia\bar{3}d$ space group.

The spectra of the Eden Mills sample (Fig. 6c) resembles that of Asbestos grossular, having 14 well-resolved peaks and two shoulders near 357 and 420 cm^{-1}. Peak positions of these grossular samples differ in accord with their compositions (i.e., almandine end-member ν values are higher than grossular end-member ν values). A small feature found in only one spectrum (not shown) near 323 cm^{-1} is likely noise, as this feature was not repeated by polarized reflectance or absorbance data (below). Thus, results on the Eden Mills grossular compare very closely with the previous data on isotropic garnets.

Because only 15 bands are observed for both birefringent grossular samples, we adopt here the previous assignments (as surmised by Hofmeister and Chopelas, 1991, from trends in the aluminous garnets) of the strong band at 241 cm^{-1} to being a doublet and of the remaining fundamental belonging to the region at 430 cm^{-1}.

Spectra from the Munam garnet (Fig. 6d) closely correlate with spectra from garnets of known isometric symmetry in terms of the number of vibrational modes, peak positions, and intensities. The 15-peak spectrum of this grandite resembles that of grossular, but peak positions for the most part lie in between those of grossular and andradite. Peak breadths are larger, as expected for an intermediate. Two weak features near 752 and 956 cm^{-1} appear to be overtones. Combinations of fundamental modes that could produce an overtone near 752 cm^{-1} are 147 + 608 = 755 cm^{-1}, 233 + 529 = 762 cm^{-1}, 288 + 459 = 747 cm^{-1}, and 378 + 378 = 756 cm^{-1}. Combinations resulting in an overtone near 956 cm^{-1} are 346 + 608 = 954 cm^{-1}, 420 + 529 = 949 cm^{-1}, and 459 + 494 = 953 cm^{-1}. Kramers-Kronig analysis shows no evidence of any more than the 17 modes expected for isometric garnet; 15 LO modes are seen in the imaginary part of $1/(\epsilon_1 + i\epsilon_2)$, whereas 16 TO modes are resolved in ϵ_2. Tentatively, modes N and P are inferred to be degenerate and assigned to the peak at 197 cm^{-1}. A definitive assignment requires data from samples of varying andradite-grossular composition so that the shift in peak positions of these modes may be accurately tracked across the binary.

Polarized reflectance

Spectra polarized at 0 and 90° with respect to extinction directions were taken from the zones shown in Figures 1–5. Examples of only four such measurements are shown, because variations were lacking.

Two pairs of polarized reflectance measurements were taken from two pieces of the andradite (Fig. 1). Although the unpolarized spectrum for the andradite has several noiselike features in the region at ~550–690 cm^{-1}, spectra obtained at both orientations of the polarizer (Fig. 7a) show a smooth curve in this region. This difference occurs because the polarized spectra were obtained using 600 scans over a sample area of ~36000 μm^2, whereas the unpolarized spectra involve one-tenth of the area but twice as many scans. Thus, the unpolarized spectra should have ~0.14 times the signal to noise ratio of the polarized sample. Other than this noisy region, no differences exist among spectra for the andradite.

Four pairs of polarized reflectance spectra were obtained from three areas of the Asbestos grossular (Fig. 2). Both the peak positions and number of peaks remain constant between the two polarized and one unpolarized spectra (Fig. 7c). Very small irregularities in low-frequency shoulders appear to be noise. Below ~200 cm^{-1} the signal to noise ratio is too low to produce reliable polarized data, whereas the signal to noise ratio for unpolarized data is high down to ~150 cm^{-1} (Fig. 7c).

For the Eden Mills grossular (Figs. 3 and 4), a total of 12 pairs of polarized reflectance spectra were taken from

→

Fig. 6. Single-crystal reflectance data from birefringent grossular-andradite. (**Top**) Raw spectrum. Labels correspond to peak positions in Table 6. (**Middle**) The dielectric function ϵ_2 and imaginary part Im $(1/\epsilon)$ obtained from Kramers-Kronig analysis. (**Bottom**) The dielectric function ϵ_1. (**a**) Andradite, Sonoma. (**b**) Grossular, Asbestos. (**c**) Grossular, Eden Mills. (**d**) Grandite, Munam. Photomicrographs of the samples and areas studied are shown in Figs. 1–5.

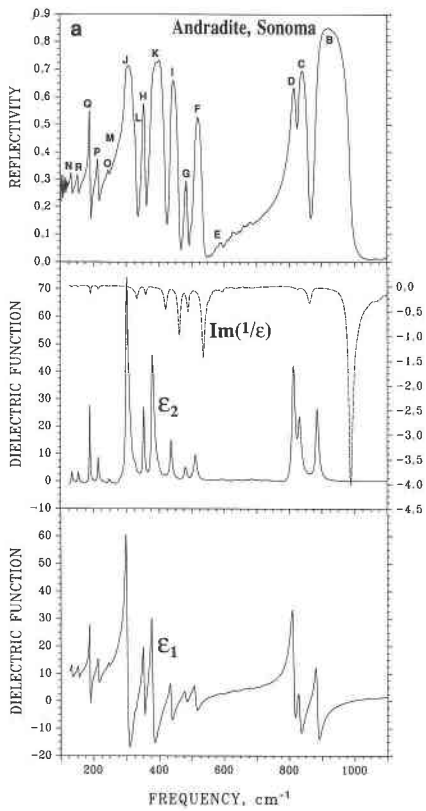
a
Andradite, Sonoma
REFLECTIVITY
DIELECTRIC FUNCTION
Im(1/ε)
ε2
ε1
FREQUENCY, cm-1

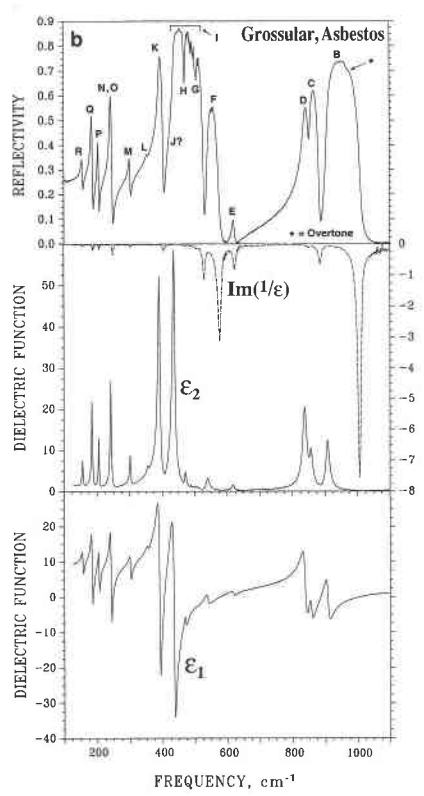
b
Grossular, Asbestos
* = Overtone
REFLECTIVITY
DIELECTRIC FUNCTION
Im(1/ε)
ε2
ε1
FREQUENCY, cm-1

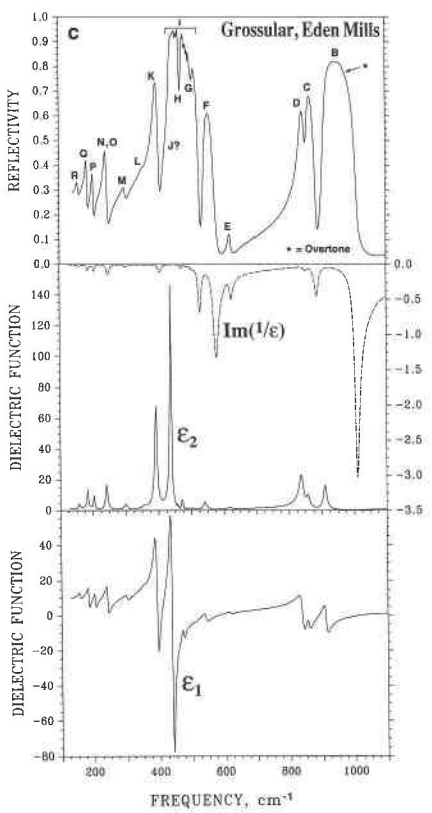
c
Grossular, Eden Mills
* = Overtone
REFLECTIVITY
DIELECTRIC FUNCTION
Im(1/ε)
ε2
ε1
FREQUENCY, cm-1

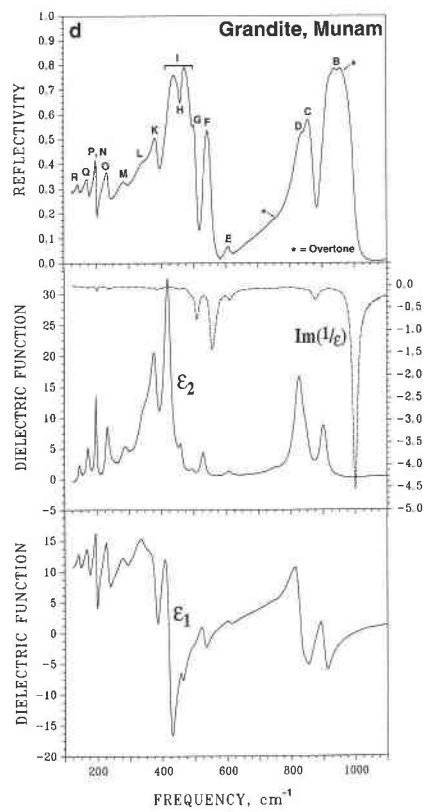
d
Grandite, Munam
* = Overtone
REFLECTIVITY
DIELECTRIC FUNCTION
Im(1/ε)
ε2
ε1
FREQUENCY, cm-1

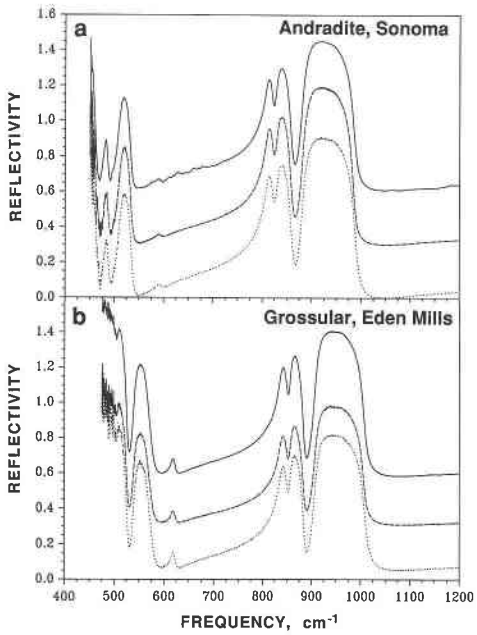

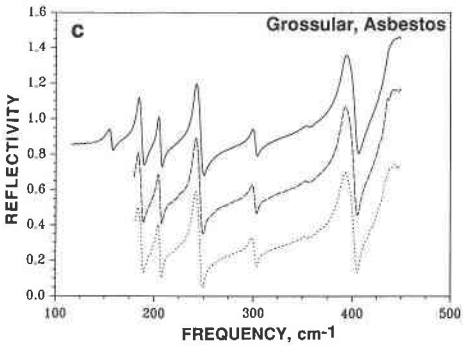

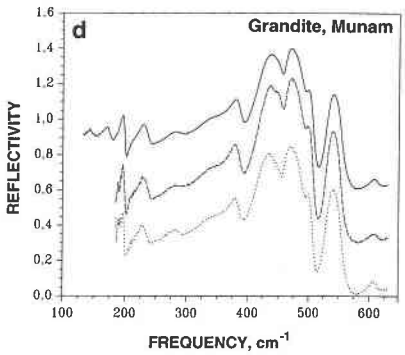

Fig. 7. Representative spatial and polarization data on birefringent garnets. Solid line = unpolarized data. Dashed line = polarized at 0° relative to extinction direction. Dotted line = polarized at 90°. (**a**) Sonoma andradite. The mid-IR unpolarized reflectance spectrum is from a different fragment than the polarized spectra. (**b**) Eden Mills grossular. These mid-IR spectra were obtained from area 1 of the sample cut to be parallel to the (110) face (Fig. 3). (**c**) Asbestos grossular. These far-IR spectra were obtained from area 2 of the sample (Fig. 2). Polarized spectra are cut off at 180 cm^{-1} because of the low signal to noise ratio below this frequency. (**d**) Munam grandite. These far-IR reflectance spectra were obtained from area 2 (Fig. 5). Noise below about 300 cm^{-1} is due to the use of a polarizing grid on a KRS-5 substrate. Other far-IR data were collected using a polyethelene substrate with a 50-cm^{-1} cutoff.

seven zones on a cut parallel to the (110) face and from five zones on a cut perpendicular to (110) on a different sample. Figure 7b shows data from one such zone. No differences exist among the various zones between spectra polarized at 0 or at 90° or between unpolarized and polarized spectra.

Pairs of polarized reflectance spectra were obtained from two areas of the Munam grandite (Fig. 5). Slight differences between each of the far-IR (Fig. 7d) and mid-IR (not shown) pairs of polarized spectra are caused by the non-normal angle of incidence and the use of S polarization for one direction, but P for the other. Lower intensity for the peaks and the presence of noise below ~300 cm^{-1} are due to reduced light levels with the polarizer. Features indicative of nonisometric symmetry were not seen.

For all samples, differences observed between the pairs of orthogonally polarized spectra are insignificant, and variations between polarized and unpolarized spectra were trivial.

Absorbance spectra

Each unpolarized absorbance spectrum (Fig. 8) resembles its reflectance counterpart, showing most, if not all, of the 17 IR modes characteristic of isometric garnets. Correspondence with the thin-film far-IR spectra of pure synthetic andradite obtained by Hofmeister and Chopelas (1991) is also excellent. In contrast, correspondence with IR powder spectra of andradite by Madon et al. (1991) is poor. First, the Madon sample appears to have significant solid solution, as indicated by the presence of the 112-cm^{-1} almandine Fe^{2+} translation (see spectra in Moore et al., 1971; and Hofmeister and Chopelas, 1991) and by the presence of only two bands in the ν_3 stretching region, as seen in Suwa and Naka's (1975) IR spectra of uvarovite-spessartine solid solutions. Second, overtones in the Madon et al. (1991) spectra are disproportionately intense compared with the fundamentals, which, in turn, led to their erroneous band assignments. Enhancement of overtones is due to the sampling of multiple particulate thicknesses with the powder method.

The TO modes dominate the absorbance spectra, and peak positions from the absorbance spectra of ultra-thin sections (less than a few micrometers) closely correspond to the TO values obtained from reflectance data (Table 6). For the thinnest sample (Eden Mills grossular), the absorption pattern most closely resembles the reflectance (Figs. 6c and 8c). Spectra from slightly thicker Asbestos grossular are similar but noisier near ~430–~510 cm^{-1},

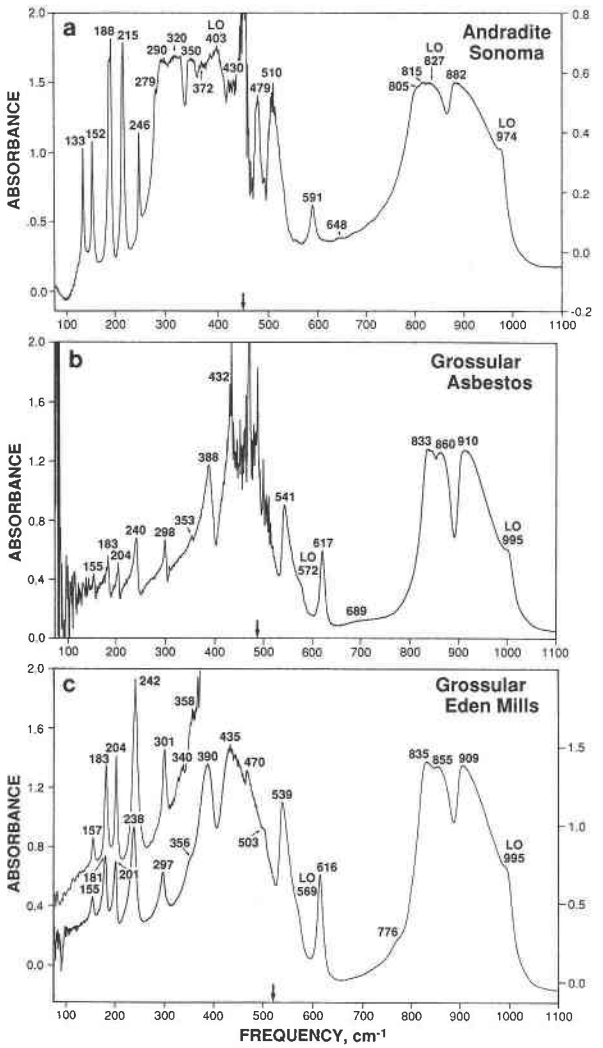

Fig. 8. Unpolarized IR absorbance spectra from single crystals of birefringent grossular-andradite. Heavy arrow at bottom indicates where spectra were merged. Noise near 400 cm^{-1} occurs because of low detector sensitivity and high IR intensity in this region. (**a**) Andradite, Sonoma. (**b**) Grossular, Asbestos. (**c**) Grossular, Eden Mills. Inset shows spectra from a thicker sample, ~4 μm thick.

where the most intense peaks occur. Absorption data were not obtained from the Munam sample because this crystal was on loan. For the andradite, significant differences exist near ~280–460 cm^{-1}; however, this approximately micrometer-thick sample is still too opaque for the highest intensity peaks to be on scale. Absorbance data in the far-IR region of andradite were obtained from a larger, thicker area (~5 μm from microscope observations) than that used in the mid-IR region. Exact thicknesses could not be established because the samples are wedged and quite thin. Previous IR data on beryl (Hofmeister et al., 1987) suggest sample thicknesses of about 1 μm.

The shapes of weakest, lowest frequency peaks of the Asbestos sample have some reflectance character. It is probable that this sample was oriented such that a component of the internal reflectance was present only for these low-absorptivity peaks because the more absorbant regions of this sample appear normal: that is, a small portion of the beam in a low-absorbance region was reflected at the exit side of the sample, was again reflected at the entrance side of the sample, and then traversed the sample once more before reaching the detector.

The highest intensity peaks (i.e., 290–450 and 430–510 cm^{-1} for andradite and the grossular, respectively, and ~800–910 cm^{-1} for all three samples), have a rounded or stubby appearance. Reasons for that are discussed after comparison with calculated peak shapes.

A few LO components are seen, as expected for a wedge-shaped or thick crystal (Berreman, 1963) and as expected from calculations of absorptivity (see below). LO modes accompany the most intense TO modes, especially for those isolated from other peaks. For example, LO components are found at 403, 827, and 974 cm^{-1} in the andradite (Fig. 8a), at 572 and 995 cm^{-1} in the Asbestos grossular (Fig. 8b), and at 569 and 995 cm^{-1} in the Eden Mills grossular (Fig. 8c). This differs significantly from powder spectra, wherein all peaks are some combination of TO and LO components.

A few weak bands in addition to the 17 fundamentals consistently occur near 600–700 cm^{-1}. These extra peaks appear to be overtones. First, such features are observed in isometric garnets: a weak band was seen at 690 cm^{-1} for An_{93} (Moore et al., 1971) and near 704 cm^{-1} for andradite of unknown composition (Madon et al., 1991). Second, their frequencies are closely matched by several pairings of fundamental frequencies. For andradite, the band at 648 cm^{-1} could be produced by 290 + 350 = 640 cm^{-1}, 279 + 372 = 651 cm^{-1}, 214 + 428 = 642 cm^{-1}, and 133 + 510 = 643 cm^{-1}. For Asbestos grossular, the band at 689 cm^{-1} could originate from 298 + 388 = 686 cm^{-1} and 155 + 541 = 696 cm^{-1}. For Eden Mills grossular, overtones at 776 cm^{-1} could be due to the pairs 356 + 430 = 786 cm^{-1}, 297 + 470 = 767 cm^{-1}, and 238 + 539 = 777 cm^{-1}.

Also, one very weak mode was at 340 cm^{-1} in absorbance for the Eden Mills sample (Fig. 8c). This is sufficiently weak to be simply noise or could originate from the 6% andradite component in this garnet. Given that two fundamentals are inferred rather than observed for grossular (Table 6), there is no reason to assume that this sole peak observed in only one of the 20 spectra acquired for Eden Mills is the manifestation of the 129 peaks expected for triclinic garnet.

Thus, no evidence exists in the absorption spectra of any additional modes besides those expected for the $Ia\bar{3}d$ space group.

Comparison of measured absorption spectra with ideal absorptivity calculated from reflectance data

Absorptivity is related to the dielectric ϵ_2 and optical n functions by

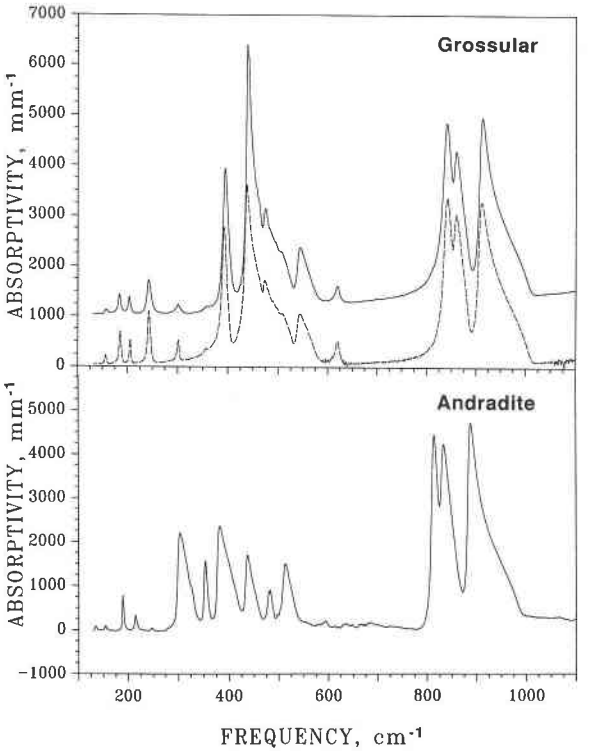

Fig. 9. Absorptivity of birefringent garnets, as calculated from unpolarized reflectance data. (**Top**) grossular; solid line is Eden Mills, dashed is Asbestos. (**Bottom**) Sonoma andradite.

$$a(\nu) = 2\pi\nu\epsilon_2(\nu)/n(\nu) \qquad (3)$$

(e.g., Wooten, 1972). Both of these functions are obtained in a Kramers-Kronig analysis of reflectivity data (e.g., Andermann et al., 1965). The resulting absorptivity (Fig. 9) represents an ideal thin sample, that is, LO modes are not intentionally included. Yet, shoulders are present at LO positions of 560 and 970 cm^{-1} in calculated absorptivity for grossular and similarly at 410 and 970 cm^{-1} for andradite, as was observed (Fig. 8).

The calculations (Fig. 9) resemble the measured absorbances (Fig. 8), particularly for the thin grossular. The rounded shapes of the three measured high-frequency stretches, compared with the sharp peak shapes of the calculations, are mainly due to the fact that a film ~ 1 μm thick is nearly opaque in this wavelength region. Occasional measurements taken during sample thinning showed that the peaks at $\sim$800–910 cm^{-1} progressed from flat plateaus to rounded plateaus to the final results of Figure 8. Further ion-milling of samples to obtain the calculated sharp peak shapes was not attempted because of the likelihood of losing samples. The rounded shapes of these peaks cannot be due to multiple peaks because the same peak profiles are seen in powder spectra of garnets for which no birefringence was reported (Moore et al., 1971), because no increase in peak width expected for overlapping peaks was seen, and because the resolution of 1 cm^{-1} used and the signal to noise ratio obtained are sufficiently high to separate multiple peaks. It is important to note that powder dispersions often show rounded peaks because of sampling various thicknesses: thus, wedging (Berreman, 1963) or irregularities in thickness could also contribute to this difference. Sharper peaks for these and other garnets can be obtained from samples compressed in a diamond-anvil cell (Lu et al., 1993; McAloon, in preparation) simply because smaller thicknesses are attained.

For the Eden Mills sample, an average thickness suggested by the comparison of calculations and measurements is 0.8 μm, and the appearance of the measured spectrum comes closest to that of the calculated absorptivity. Absorption measurements of Asbestos grossular are similar to the calculated intensity pattern. The average thickness estimated by comparison of the bands at 541 cm^{-1} is 0.9 μm. For the andradite, a large and relatively thick area was needed to achieve reasonable signal to noise levels for the far-IR region (Fig. 8a). Obviously, this sample is nearly opaque from 300 to 430 cm^{-1}, and the apparent peak shapes are not representative. Comparison of measured absorbance for the 152-cm^{-1} mode with calculated absorptivities suggests that the andradite far-IR section overall is 8 μm thick, whereas a comparison using the 510-cm^{-1} peak suggests that the mid-IR section is thinner, at $\sim$0.4 μm. We place little confidence in the thickness obtained from mid-IR data because absorbance goes below zero at high frequency because of the lenslike behavior of this wedged sample. The decrease in thickness from the andradite to the Eden Mills sample is corroborated by microscope observations.

The close approach of measured absorbance to absorptivity calculated from the reflectance data indicates that no hidden peaks exist for any of the three near end-members. We infer that all fundamentals were revealed by the reflectivity spectrum of the Munam grandite.

What is the space group of the four birefringent garnets?

The IR data indicate that these four birefringent garnet samples crystallized in space group $Ia\bar{3}d$ in that (1) the number of peaks appropriate to the isometric structure was seen in reflectivity and absorbance, and (2) no polarization differences were observed. We emphasize that the possible existence of one extra peak in the overtone region or one noisy peak at 340 cm^{-1} in one spectrum of Eden Mills garnet are insufficient evidence of the 112 extra bands expected for $I\bar{1}$ or even of the 33 extra bands expected for more symmetrical, ordered garnets such as those with space group $I4_1/acd$.

Supporting evidence is found in Raman spectra of Jeffrey mine grossular being as expected for isometric garnet (Hofmeister and Chopelas, 1991). The sample was marginally birefringent because of its small size, but large samples from this locality have obvious optical anomalies. Nuclear magnetic resonance (^{27}Al MAS NMR) measurements on a sample of Asbestos grossular were nearly

identical to a simulation using single-crystal NMR parameters obtained from isometric grossular (B. Phillips, 1992 personal communication).

Space group $Ia\bar{3}d$ contradicts previous crystallographic refinements of grandites (Takéuchi et al., 1982; Allen and Buseck, 1988; Kingma and Downs, 1989), from which space group $I\bar{1}$ or *Fddd* was deduced and attributed to the ordering of cations in the octahedral or dodecahedral sites. We examine three alternative explanations: (1) IR spectroscopy is not sensitive enough to reveal the small distortions seen by crystallography; (2) IR spectroscopy is insufficiently sensitive to reveal the partial Al-Fe ordering inferred by crystallography; (3) birefringence is caused by strain in these samples instead of ordering.

Hypothesis 1. Three observations indicate that small distortions in the unit-cell dimensions of 0.109% for Eden Mills (based on the $I\bar{1}$ refinement by Allen and Buseck, 1988) and 0.023% for the Munam sample (based on values given by Takéuchi et al., 1982) should be resolved by IR spectroscopy if such distortions exist. First, IR spectra of a large number of slightly distorted samples show increased numbers of bands caused by lowered symmetry. Second, the most closely related example is majorite garnet, which has only a 0.18% distortion from isometric symmetry (based on values from Angel et al., 1989), and shows 19 bands over 400–1200 cm^{-1}, many of which are strong, compared with eight for structurally and chemically similar pyrope (McMillan et al., 1989). The number is consistent with 21 internal modes, rotations, and translations of $^{[6]}Si$ for the E_u symmetry in tetragonal garnet. The weaker (mostly A_{2u}) modes are not seen, as is expected and common for a powder spectrum. Third, the point at which IR spectroscopy is no longer able to detect symmetry differences due to distortion is attained when the excursion of the atoms during the vibration exceeds the distortion. Obviously, such distortions also cannot be observed in crystallographic refinements, other than in the magnitude of the thermal ellipsoids. An example is the α- to β-quartz transition at 573 °C. Crystallography has shown that β quartz is hexagonal with six SiO_4 tetrahedra in a ringlike configuration and that α quartz is either its right- or left-hand distortion. These constitute a twin pair by rotation. TEM studies by van Tendeloo et al. (1976) have shown that the high temperature polymorph is a space and time average of these Dauphiné microtwins. Thus, the β structure oscillates between the α enantiomorphs. IR spectroscopic measurements are in perfect agreement: the spectra of the lower symmetry structure remain intact up to the transition point and show mode softening, whereas frequencies of β above 573 °C are nearly temperature independent (Gervais and Piriou, 1975), and the internal rotational mode E_1 is implicated in the phase transition (Iishi, 1978).

Hypothesis 2. For the case at hand, the garnet structure may not necessarily be altered by distortion: Kingma and Downs (1989) have shown that although the andradite unit cell remains isometric as measured, symmetry elements are lost during cation ordering. It is not clear from examples or theory whether such partial ordering of Al-Fe can be detected by IR spectroscopy.

Thus, IR spectra provide strong evidence that the unit cell is isometric in shape, but neither prove nor disprove that symmetry elements are lost through partial ordering.

Hypothesis 3. If strain is present, as proposed by Chase and Lefever (1960), then the discrepancy between spectroscopic and crystallographic structural determinations is attributed to sampling requirements. Coherent diffraction of X-rays requires a multiplicity of juxtaposed unit cells: in practice, several hundreds, perhaps a thousand, contiguous unit cells are needed. In contrast, spectroscopy can yield information for completely disordered substances, such as glasses, or on isolated bonds, such as those of gases or solutes (e.g., White, 1974). Vibrational spectroscopy provides information on amorphous materials because vibrations are essentially nearest neighbor interactions. Thus, for spectroscopy none of the units need be interconnected, whereas for crystallography the Bragg condition must be met. A relevant example is the cordierite transformation: IR spectra showed that hexagonal cordierite crystals were present after 0.5 min of annealing, but X-ray data showed no evidence of the orthorhombic to hexagonal transformation until after 100 h, at which point transmission electron microscopy (TEM) indicated twinning domains of 1000 Å (Putnis and Bish, 1983). It is clear that the size minimum for X-ray diffraction is orders of magnitude larger than that required for IR. For the case at hand, the lower symmetry indicated by crystallography could result from misalignment within the ~1000 isometric unit cells sampled, i.e., strain. This conclusion is supported by no indication of ordering either in powder diffraction patterns or in the high-resolution TEM study of Allen and Buseck (1988) over a 10-μm aperture, in contrast to the detection of ordering in conventional diffraction studies of crystals 80 μm in length. Strain could have been released while grinding the samples into grain sizes of 1–3 μm, or it could occur over a scale larger than 10 μm.

Origin of birefringence

Several hypotheses explaining optical anomalies in garnets have been proposed (e.g., Allen and Buseck, 1988; Kingma and Downs, 1989). These include (1) lattice mismatch at grain, compositional or twin boundaries resulting in strain (Chase and Lefever, 1960; Lessing and Standish, 1973; Kitamura and Komatsu, 1978); (2) partial ordering of Al and Fe^{3+} among the octahedra (Takéuchi et al., 1982; Allen and Buseck, 1988; Kingma and Downs, 1989) or partial ordering of Ca and Fe^{2+} among the dodecahedral sites (Allen and Buseck, 1988; Griffen et al., 1992); (3) magneto-optic effects due to substitution of rare-earth cations for Ca (Blanc and Maisonneuve, 1973); (4) nonisometric distribution of OH^- groups (Rossman and Aines, 1986); and (5) twinning (Ingerson and Barksdale, 1943). Although hypotheses 3–5 may affect some garnets, these solutions are unlikely to be comprehensive, as follows.

Replacement of Ca by rare-earth cations is an interesting hypothesis but is unsupported by data. It seems unlikely that natural birefringent garnets from such diverse settings as skarns, schists, pegmatites, and peridotites, which have a wide range of composition including uvarovite, pyralspites, grossular almandine (Hofmeister et al., in preparation), and grossular pyralspites (Griffen et al., 1992), would all contain rare-earth cations in the dodecahedral site. Moreover, occurrence of birefringence in synthetic phases such as YAG-YIG solid solutions (Kitamura and Komatsu, 1978) and other garnets such as $Yb_3Ga_5O_{12}$ (Chase and Lefever, 1960), which should be pure, suggests that minor elements are not responsible. If rare-earth elements were responsible for anomalous optics, it seems reasonable that garnets with large concentrations should exhibit very strong birefringence. Yet, samples having dodecahedral sites filled with rare-earth elements are weakly birefringent (Chase and Lefever, 1960; Kitamura and Komatsu, 1978), suggesting that these elements are not responsible. The wide range of compositions for natural and synthetic garnets exhibiting birefringence implies that the cause is not one simple chemical entity.

The directionality of the OH^- vibrations is not directly correlated with the optics (Allen and Buseck, 1988), nor do all birefringent grandites have OH^- distributed nonisometrically (Rossman and Aines, 1986). The presence of H_2O is not essential because OH was removed by heating samples to 800 °C, yet the birefringence remained (Allen and Buseck, 1988). H_2O is also not expected to be incorporated in garnets grown in fluxes at 1250 °C (Chase and Lefever, 1960; Kitamura and Komatsu, 1978). Birefringence in andradite weakens but remains after heating to 1225 °C (Ingerson and Barksdale, 1943), which should be sufficient for dehydration. Mantle-derived garnets are sometimes birefringent (Hofmeister et al., in preparation), yet they are fairly dry, with <0.25 wt% H_2O (Aines and Rossman, 1984). Thus, OH^- is not likely a universal cause of birefringence.

Twinning cannot be essential because it is not observed in all birefringent garnets.

Strain incorporated during growth or partial ordering of cations are viable causes of optical anisotropy in garnets. It may be that both are present or that some garnets are ordered whereas others are strained. We prefer an origin in strain over Al-Fe ordering for the following reasons:

The wavy extinction of many samples suggests strain. Extended defects such as stacking faults and dislocations were observed to be concentrated near sector boundaries in the Eden Mills grossular (Allen and Buseck, 1988). Presence of strain readily accounts for the determination of different space groups through spectroscopy and crystallography, as discussed in the previous section. Strain could also explain variable orientational anisotropy of OH^- groups (e.g., Rossman and Aines, 1991). Strain is also compatible with the high temperatures needed to remove birefringence.

Strain-related optical anomalies are known in other minerals. Although diamond is generally accepted as isometric in structure, birefringence is a common feature of this mineral. Of 5000 crystals and fragments studied by Tolansky (1966), not a single one was optically isotropic. This anisotropism is generally thought to have arisen from strain, which has been attributed to such factors as mechanical stress (Friedel, 1924), changes in chemical composition distinguishing Type I diamond from Type II (Tolansky, 1966), and the presence of inclusions of N platelets (Seal, 1966). Birefringence in diamond is well known to workers using diamond anvils in high-pressure studies; the pattern of birefringence changes as a function of pressure (Seal, 1984). Similarly, quartz can be distinctly biaxial with $2V$ as high as 10° and can possess undulatory extinction: both effects are generally eliminated if later recrystallization occurs and are attributed to strain (see summaries by Sosman, 1965; and Deer et al., 1978).

Two tests would help to differentiate strain from ordering as an origin of birefringence in garnet. First, the dependence of the diffractions indicating nonisometric symmetry should be measured as a function of crystal size. Existing TEM data indicate that small samples, ~ 10 μm, are isometric. If a detection of lowered symmetry requires a minimum crystal size that contains a multitude of unit cells, then it is impossible that ordering is the cause. Second, if ordering is the origin, then it may be possible to regain birefringence by annealing the samples slightly below the temperature at which birefringence is removed. Care must be taken, as the natural samples often become opaque rather than isotropic upon heating.

Conclusions

We have shown that all of the IR fundamentals can be resolved in absorption spectra from ion-milled garnets. The agreement with reflectance spectra is excellent. This approach provides measurements of the TO modes, rather than an indeterminant combination of LO and TO modes, as in the powder method.

The IR positions and intensities reported by Hofmeister and Chopelas (1991) for andradite and grossular are generally confirmed. This study resolved all 17 modes for andradite (previously one peak was inferred). The two modes inferred previously for grossular were not clearly resolved.

Acknowledgments

This paper represents B.P.M.'s senior thesis. We express our thanks to F.M. Allen (Engelhard Company, New Jersey), P.R. Buseck (Arizona State University), J.W. Downs (Ohio State University), K.J. Kingma (Johns Hopkins University), and G.R. Rossman (California Institute of Technology) for helpful discussions and generosity in providing samples of birefringent garnets. Discussion with B.L. Phillips (Lawrence Livermore National Laboratory) was beneficial. H.W. Green (U.C. Davis) generously allowed us to use his dimpler. N. Winter gave valuable advice and assistance during sample preparation, and J. Fong and M. Graziose helped with illustrations. B.P.M. thanks T. Fagan, R. Lu, and T. Young for advice and insight regarding IR spectroscopy. Critical reviews by D.T. Griffen (Brigham Young University), G.R. Rossman, and W.B. White (Pennsylvania State University) improved the manuscript. Support was provided

by the David and Lucile Packard Foundation and by NSF grant EAR-88-16531, with a Research for Undergraduates supplement.

References cited

Aines, R.D., and Rossman, G.R. (1984) The hydrous component in garnets: Pyralspites. American Mineralogist, 69, 1116–1126.

Allen, F.M., and Buseck, P.R. (1988) XRD, FTIR, and TEM studies of optically anisotropic grossular garnets. American Mineralogist, 73, 568–584.

Andermann, G., Caron, A., and Dows, D.A. (1965) Kramers-Kronig dispersion analysis of infrared reflectance bands. Journal of the Optical Society of America, 55, 1210–1216.

Angel, R.J., Finger, L.W., Hazen, R.M., Kanzaki, M., Weidner, D.J., Liebermann, R.C., and Veblen, D.R. (1989) Structure and twinning of single-crystal $MgSiO_3$ garnet synthesized at 17 GPa and 1800 °C. American Mineralogist, 74, 509–512.

Berreman, D.W. (1963) Infrared absorption at longitudinal optic frequency in cubic crystal films. Physical Review, 130, 2193–2198.

Blanc, Y., and Maisonneuve, J. (1973) Sur la birefringence des grenats calciques. Bulletin de la Société française de Mineralogie et de Cristallographie, 96, 320–321.

Chase, A.B., and Lefever, R.A. (1960) Birefringence of synthetic garnets. American Mineralogist, 45, 1126–1129.

Deer, W.A., Howie, R.A., and Zussman, J. (1978) An introduction to the rock-forming minerals, 528 p. Longman, London.

Euler, F., and Bruce, J.A. (1965) Oxygen coordinates of compounds with garnet structure. Acta Crystallographica, 19, 971–978.

Friedel, G. (1924) Sur la birefringence du diamant. Bulletin de la Société française de Mineralogie et de Cristallographie, 47, 60–94.

Gervais, F., and Piriou, B. (1975) Temperature dependence of transverse and longitudinal optic modes in the α and β phases of quartz. Physical Review, B11, 3944–3950.

Griffen, D.T., Hatch, D.M., Phillips, W.R., and Kulaksiz, S. (1992) Crystal chemistry and symmetry of a birefringent tetragonal $pyralspite_{75}$-$grandite_{25}$ garnet. American Mineralogist, 77, 399–406.

Hatch, D.M., and Griffen, D.T. (1989) Phase transitions in the grandite garnets. American Mineralogist, 74, 151–159.

Hofmeister, A.M., and Chopelas, A. (1991) Vibrational spectroscopy of end-member silicate garnets. Physics and Chemistry of Minerals, 17, 503–526.

Hofmeister, A.M., Hoering, T.C., and Virgo, D. (1987) Vibrational spectra of beryllium aluminosilicates: Heat capacity calculations. Physics and Chemistry of Minerals, 14, 205–224.

Hurrell, J.P., Porto, S.P.S., Chang, I.F., Mitra, S.S., and Bauman, R.P. (1968) Optical phonons of yttrium aluminum garnet. Physical Review, 173, 851–856.

Iishi, K. (1978) Lattice dynamical study of the α-β quartz phase transition. American Mineralogist, 63, 1190–1197.

Ingerson, E., and Barksdale, J.D. (1943) Iridescent garnet from the Adelaide mining district, Nevada. American Mineralogist, 28, 303–312.

Jackson, J.D. (1975) Classical electrodynamics, 848 p. Wiley, New York.

Kieffer, S.W. (1979) Thermodynamics and lattice vibrations of minerals. III. Lattice dynamics and an approximation for minerals with application to simple substances and framework substances. Reviews of Geophysics and Space Physics, 17, 35–59.

Kingma, K.J., and Downs, J.W. (1989) Crystal-structure analysis of a birefringent andradite. American Mineralogist, 74, 1307–1316.

Kitamura, K., and Komatsu, H. (1978) Optical anisotropy associated with growth striation of yttrium garnet, $Y_3(Al,Fe)_5O_{12}$. Kristallographie und Technik, 13, 811–816.

Lessing, P., and Standish, R.P. (1973) Zoned garnet from Crested Butte, Colorado. American Mineralogist, 58, 840–842.

Lu, R., Jackson, K.D., and Hofmeister, A.M. (1993) Thin-film infrared spectra from solid solutions of spessartine and yttrium aluminum garnet. Canadian Mineralogist, in press.

Madon, M., Ibarguchi, J.I.G., Via, J., and Girardeau, J. (1991) Characterization and thermodynamic properties of andradite, $Ca_3Fe_2Si_3O_{12}$. American Mineralogist, 76, 1249–1260.

McMillan, P., and Hofmeister, A.M. (1988) Infrared and Raman spectroscopy. In Mineralogical Society of America Reviews in Mineralogy, 18, 99–160.

McMillan, P., Akaogi, M., Ohtani, E., Williams, Q., Nieman, R., and Sato, R. (1989) Cation disorder in garnets along the $Mg_3Al_2Si_3O_{12}$-$Mg_4Si_4O_{12}$ join: An infrared, Raman and NMR study. Physics and Chemistry of Minerals, 16, 428–435.

Moore, R.K., White, W.B., and Long, T.V. (1971) Vibrational spectra of the common silicates. I. The garnets. American Mineralogist, 56, 54–71.

Novak, G.A., and Gibbs, G.V. (1971) The crystal chemistry of the silicate garnets. American Mineralogist, 56, 791–825.

Putnis, A., and Bish, D.L. (1983) The mechanism and kinetics of Al,Si ordering in Mg-cordierite. American Mineralogist, 68, 60–65.

Rossman, G.R., and Aines, R.D. (1986) Birefringent garnet from Asbestos, Quebec, Canada. American Mineralogist, 71, 779–780.

——— (1991) The hydrous components in garnets: Grossular-hydrogrossular. American Mineralogist, 76, 1153–1164.

Seal, M. (1966) Inclusions, birefringence and structure in natural diamonds. Nature, 212, 1528–1531.

——— (1984) Diamond anvils. High Temperatures–High Pressures, 16, 573–579.

Sosman, R.B. (1965) The phases of silica, 388 p. Rutgers University Press, New Brunswick, New Jersey.

Spitzer, W.G., Miller, R.C., Kleinman, D.A., Howarth, L.E. (1962) Far-infrared dielectric dispersion in $BaTiO_3$, $SrTiO_3$, and TiO_2. Physical Review, 126, 1710–1721.

Suwa, Y., and Naka, S. (1975) Infrared spectra of the solid solution between uvarovite and spessartine. American Mineralogist, 60, 1125–1126.

Takéuchi, Y., Haga, N., Umizu, S., and Sato, G. (1982) The derivative structure of silicate garnets in grandite. Zeitschrift für Kristallographie, 158, 53–99.

Tarte, P. (1965) Etude expérimentale et interprétation du spectre infrarouge des silicates et des germanates: Application à des problèmes structuraux relatifs à l'état solide. In Académie royale de Bruxelles classe des sciences mémoires, vol. 35, 260 p. Palais des Académies, Brussels.

Tighe, N.J. (1976) Experimental techniques. In H.-R. Wenk, Ed., Electron microscopy in mineralogy, p. 144–171. Springer-Verlag, Berlin.

Tolansky, S. (1966) Birefringence of diamond. Nature, 211, 158–160.

van Tendeloo, G., van Landuyt, J., and Amelinckx, S. (1976) The α-β-phase transition in quartz and $AlPO_4$ as studied by electron microscopy and diffraction. Physica Status Solidi A, 33, 723–735.

White, W. (1974) Order-disorder effects. In V.C. Farmer, Ed., The infrared spectra of minerals, p. 876–110. Mineralogical Society, London.

Wooten, F. (1972) Optical properties of solids, 260 p. Academic, San Diego, California.

Manuscript received September 30, 1991
Manuscript accepted April 25, 1993